Geol. Mag. **139** (5), *2002, pp. 541–558.* © *2002 Cambridge University Press*
DOI: 10.1017/S0016756802006775 *Printed in the United Kingdom*

Geochemistry, tectonomagmatic origin and chemical correlation of altered Carboniferous–Permian fallout ash tuffs in southwestern Germany

STEPHAN KÖNIGER* & VOLKER LORENZ

Institut für Geologie, Julius-Maximilians-Universität Würzburg, Pleicherwall 1, D-97070 Würzburg, Germany

(*Received* 3 April 2002; *accepted* 10 June 2002)

Abstract – Thin, but laterally widespread, fallout ash tuff layers interbedded with complex fluvio-lacustrine successions of the Carboniferous–Permian late Variscan intermontane Saar–Nahe Basin in southwestern Germany provide important tephrostratigraphic markers in the purely continental depositional setting. The tuffs are rhyolitic to rhyodacitic and indicate geochemical affinities to Moldanubian Variscan S-type granitoids. The volcanic ashes are suggested to have been derived from the general region of the central and northern Black Forest (southwestern Germany) and the northern Vosges (eastern France) at 100–150 km distance south of the Saar–Nahe Basin. Six tuff beds from the Jeckenbach and Odernheim subformations (Meisenheim Formation, Glan Group) have been correlated within the basin over a distance of 50 km by mapping and whole-rock geochemical fingerprinting. In each subformation, three tuffs can be well distinguished using geochemical discriminant function analysis. Additional comparisons of trace and rare-earth element contents provide further criteria for the differentiation of individual tuff beds. These discriminations show that the tuffs have unique chemical fingerprints, probably reflecting differences in the original composition of the parent volcanic tephra. Thus, chemical differences between the tephrostratigraphic markers are geologically significant and provide a powerful tool for establishing tuff layer identification and correlation within the complex sedimentary sequence of the Saar–Nahe Basin. They also provide clues to the tectonomagmatic settings of the source volcanoes.

Keywords: tuff, pyroclastics, Permian, Saar–Nahe Basin, geochemistry, geochemical indicators.

1. Introduction

Explosive volcanic eruptions can produce large amounts of fine-grained pyroclastic material which spread laterally at tropospheric and stratospheric altitudes by wind drift. Characteristic features of the resulting volcanic fallout ash deposits are their (1) lateral continuity, (2) generally exponentially decreasing thickness away from the source, (3) comparatively high sedimentation rates and (4) isochronous deposition. However, within specific regions they show relatively constant thicknesses. Such fall-derived pyroclastic beds tend to mantle the pre-eruptive topography of the depositional surface independent of the environmental setting (Fisher & Schmincke, 1984; Cas & Wright, 1987).

Carboniferous–Permian sediments in Central Europe contain numerous fine ash tuff beds. They have enormous stratigraphic potential since they form excellent isochronous chronostratigraphic marker horizons within rock sequences characterized by complex facies relationships, especially within continental successions as, for example, in the Saar–Nahe Basin in southwestern Germany. Such tuff layers may enable correlations within a basin, between basins, and to potential source regions. Due to the age of these tephrostratigraphic markers, landmarks like ancient volcanoes which would indicate possible source areas of the volcanic ash no longer exist. For this reason, the geochemical composition of tuff horizons, although altered, can be used to determine the tectonomagmatic derivation of the ash by applying tectonomagmatic discrimination diagrams, such as from Pearce, Harris & Tindle (1984) or Harris, Pearce & Tindle (1986). These can provide clues to potential source regions.

Although thin ash tuff horizons are known to occur widely in the Saar–Nahe Basin (e.g. Heim, 1960, 1961, 1970; Boy, Meckert & Schindler, 1990; Königer, 1999, 2000), their usefulness in stratigraphy has been limited to comparatively short-range correlations due to the difficulty of distinguishing one bed from another. Their overall mineralogy and petrological features are similar and they tend to vary in thickness, colour, texture and general appearance as much laterally within individual horizons as between them. Chemical fingerprinting based on whole-rock analyses has been successively used in tracing and correlating Cenozoic tephra layers in North America (Borchardt, Harward & Schmitt, 1971; Borchardt, Norgren & Harward, 1973; Randle, Goles & Kittleman, 1971; Westgate &

* Author for correspondence: stephan.koeniger@t-online.de

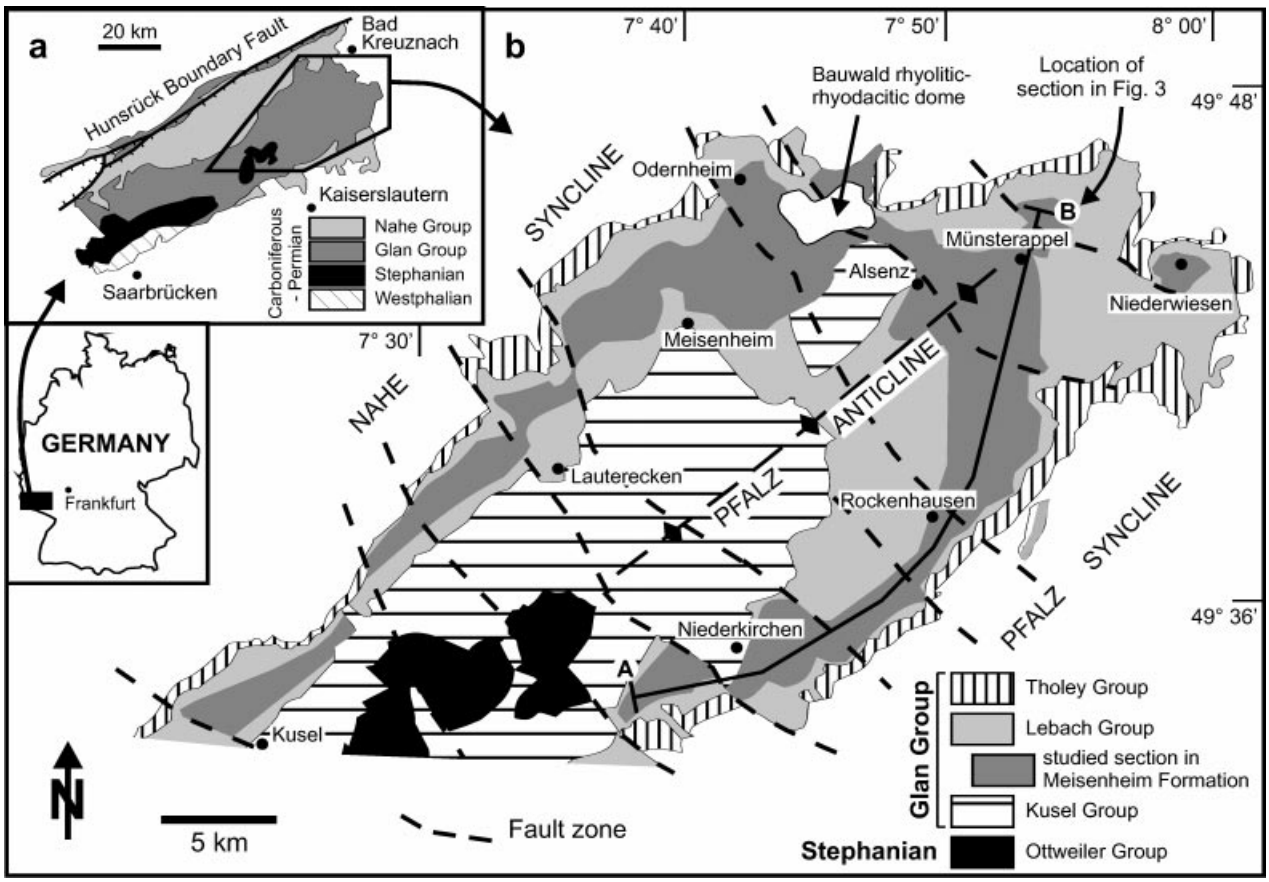

Figure 1. (a) Distribution of Upper Carboniferous and Lower Permian strata in the Saar–Nahe Basin and location of the study area; (b) distribution of the Glan Group (replacing the former Kusel, Lebach and Tholey groups) in the northeastern part of the basin. Major structural elements include NE–SW trending synclines and anticlines.

Fulton, 1975; Westgate, Christiansen & Boellstorff, 1977), Ordovician K-bentonites in North America (Huff, 1983; Kolata, Frost & Huff, 1986, 1987; Huff & Kolata, 1989; Kolata, Huff & Bergström, 1996; Huff *et al.* 1996), and Silurian K-bentonites in Britain (Huff *et al.* 1991; Huff, Morgan & Rundle, 1996) and northern Europe (Huff *et al.* 1998). This method offers a possible means of differentiating Carboniferous–Permian (altered) tuff beds in Central Europe, although some caution must be taken in evaluating chemical data from them because of post-depositional alteration effects on the former volcanic ash layers.

Due to intense alteration, many tuff horizons in the Saar–Nahe Basin were formerly described as 'tonsteins' (kaolinite-rich mudstones) (e.g. Heim, 1960, 1961, 1970) even if their volcanic origin had already been established. Following standard volcanological nomenclature, the altered horizons examined in this study are termed 'tuffs' because of their original formation as volcanic fallout ash layers which are now indurated, although other workers might name them 'bentonites'. For a discussion of these definitions, see Fisher & Schmincke (1984).

In this paper, the geochemical composition of a series of volcaniclastic horizons in the Saar–Nahe Basin is documented and compared with published data of magmatic rocks of potential source areas. It is our aim to discuss (1) their host magmas, (2) the tectonomagmatic origin and source regions of the volcanic ash, and (3) the discrimination and correlation of individual tuff beds within the basin based on whole-rock chemical fingerprinting.

2. Geological setting

The Saar–Nahe Basin in southwestern Germany extends northeast–southwestward from about 40 km west of Frankfurt to the French–German border near Saarbrücken (Fig. 1). With its exposed dimensions of 120×40 km, it is one of the largest of about 70 intermontane basins which developed during the late-orogenic (Late Carboniferous–Early Permian) extension of the Variscan orogenic belt (Lorenz & Nicholls, 1976, 1984). The basin fill comprises exclusively continental sediments with a preserved thickness of about 6500 m (Henk, 1992). Deposition started at the Namurian/Westphalian boundary (Upper Bashkirian) and continued until late Early Permian times, recording a shift from a humid towards a semi-arid climate over more than 20 m.y. (Lippolt, Hess & Burger, 1984; Lippolt & Hess, 1989) during continuous northward drift of the basin (Ziegler, 1990). Towards the south,

https://doi.org/10.1017/S0016756802006775 Published online by Cambridge University Press

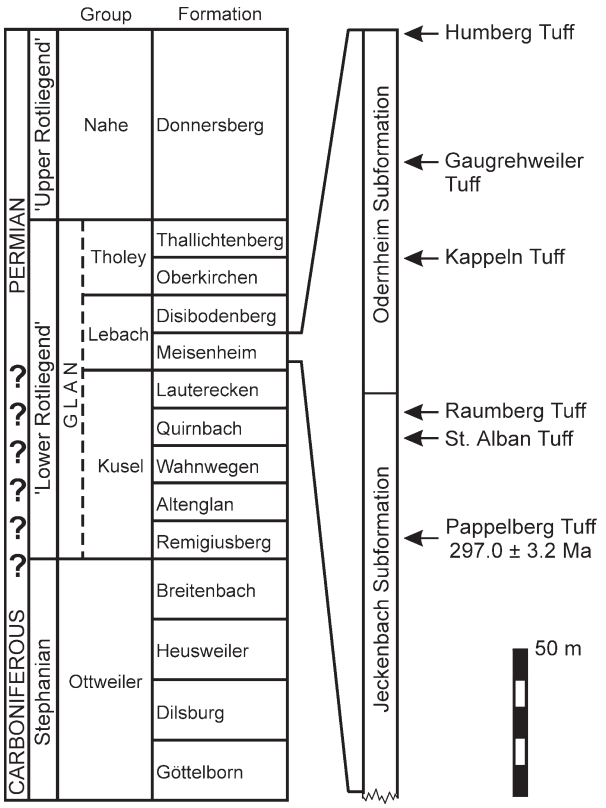

Figure 2. Generalized Stephanian and 'Rotliegend' stratigraphy of the Saar–Nahe Basin illustrating the stratigraphic positions of the studied section and important tephrostratigraphic marker horizons of the Meisenheim Formation. The question marks indicate the uncertain position of the Carboniferous/Permian boundary. The age of the Pappelberg Tuff is taken from Königer *et al.* (2002).

east and west of the basin, sediments of Triassic and Tertiary age cover large areas of the Carboniferous–Permian basin fill, and the true basin dimensions are only known from a few boreholes and seismic lines. Seismic sections across the Saar–Nahe Basin and the asymmetric distribution of sediment thicknesses and facies reveal the half-graben structure of the basin (Henk, 1993). The main basin bounding fault is a southeastward dipping detachment which coincides with the surface trace of the Hunsrück Boundary Fault at the northwestern basin margin (Fig. 1a). The intrabasinal structural framework comprises NW–SE-trending oblique slip transfer faults (Stollhofen, 1998) and large-scale synclinal and anticlinal structures running NE–SW subparallel to the basin margins (Fig. 1b). The study area is located in the northeastern part of the Saar–Nahe Basin, covering about 1000 km^2, and includes the northeastern part of the Pfalz Anticline (Fig. 1a).

3. Lithostratigraphy and radiometric age

This paper deals with a sedimentary succession in the middle part of the Glan Group (former 'Lower Rotliegend'; Fig. 2; cf. Boy & Fichter, 1982), embracing parts of the Meisenheim Formation (Jeckenbach and Odernheim subformations; cf. Haneke & Kremb, 1998). The Glan Group comprises the former Kusel, Lebach and Tholey groups (Boy & Fichter, 1982).

The examined succession is characterized by purely continental, laterally variable fluvio-lacustrine sediments revealing complex thickness and facies patterns. Figure 3 shows the complex architecture of the sequence resulting from synsedimentary tectonics. Lateral intrabasinal correlations are difficult when based only on litho- and biostratigraphic aspects. The facies associations of the sedimentary succession are organized into fluvio-lacustrine, transgressive–regressive cycles (Königer & Stollhofen, 2001). The section shows the development of three major facies assemblages which are arranged in combined upward-fining and upward-coarsening cycles: (1) an offshore-lacustrine facies association, (2) a prodelta to delta front facies association, and (3) a delta plain facies association. A detailed description of the lithofacies is given by Königer & Stollhofen (2001).

More than 40 ash tuff horizons can be distinguished within the studied 260–370 m thick section (Königer, 2000), but only six represent important tephrostratigraphic markers, due to their wide and almost continuous lateral distribution within the Saar–Nahe Basin. These are the Pappelberg, St Alban, Raumberg, Kappeln, Gaugrehweiler and Humberg tuffs (Fig. 2). Other horizons like the Jeckenbach, Hesselberg and Odernheim tuffs (see Fig. 3) have a more restricted occurrence but nevertheless can help locally to decode the stratigraphic sequence. Most of the tephrostratigraphic nomenclature has been derived from Boy, Meckert & Schindler (1990), except for the St Alban Tuff (Haneke & Stollhofen, 1994) and Gaugrehweiler Tuff (Königer, Stollhofen & Lorenz, 1995).

The Pappelberg Tuff in the lower part of the Meisenheim Formation has been dated at 297.0 ± 3.2 Ma by U–Pb SHRIMP dating of zircons (Fig. 2; Königer *et al.* 2002). Taking the age of the Carboniferous/Permian boundary as 296 Ma (Menning, 1995; Menning *et al.* 1997), the Meisenheim Formation approximately corresponds to the Carboniferous/Permian boundary. Thus, the Meisenheim Formation is considered to represent the uppermost Carboniferous to lowermost Permian succession in the Saar–Nahe Basin (Königer *et al.* 2002).

4. Tephrostratigraphic horizons of the Meisenheim Formation

4.a. Occurrence and deposition

On the basis of their physical properties (e.g. light colours, hardness due to secondary silicification, internal structures, polyhedral disintegration of hand specimen) and compositional characteristics, the tephrostratigraphic horizons of the Meisenheim

https://doi.org/10.1017/S0016756802006775 Published online by Cambridge University Press

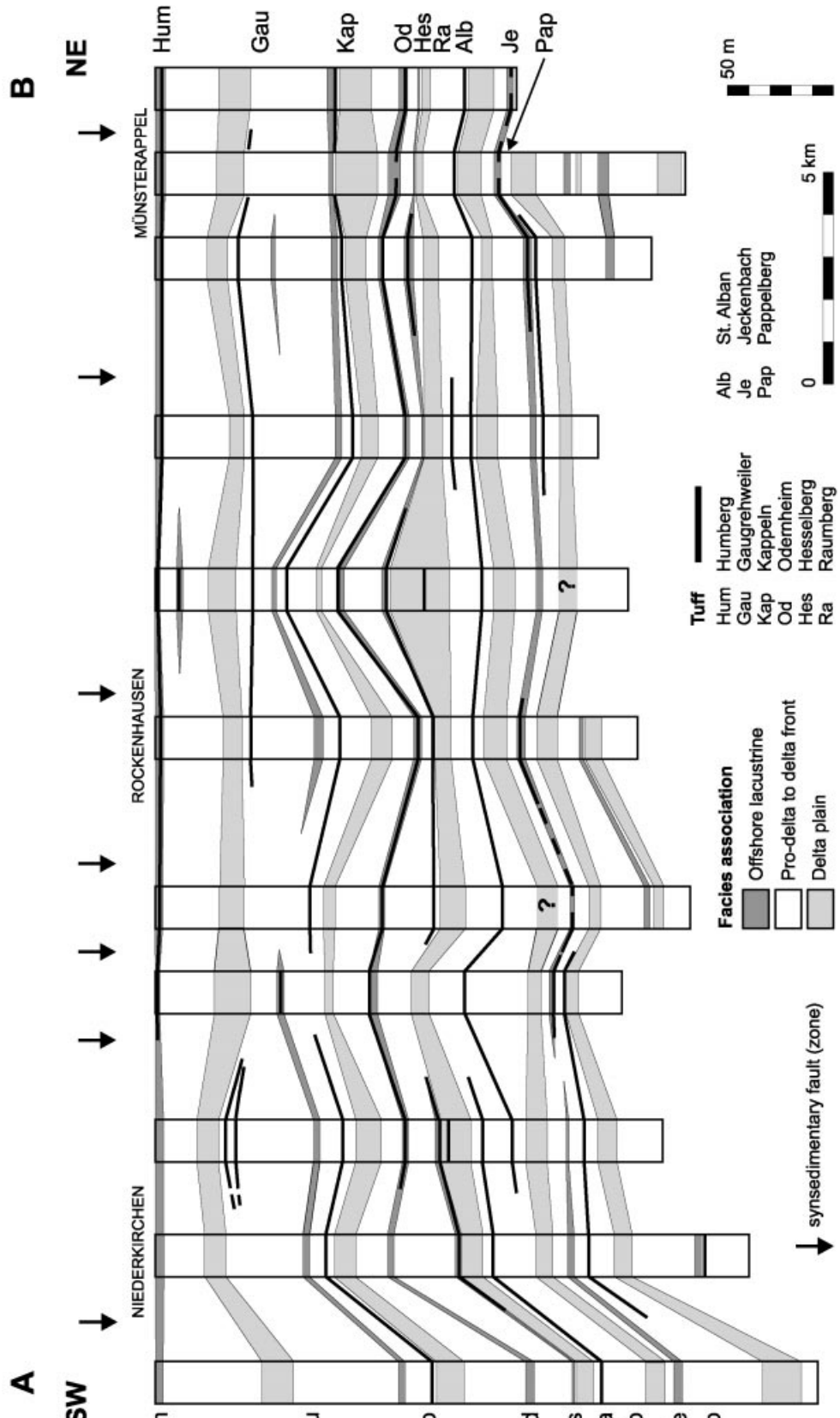

Figure 3. SW–NE section documenting the complex architecture of the Meisenheim Formation and the lithostratigraphic positions of the major tuff horizons along the SE-flank of the Pfalz Anticline (for location see Fig. 1b). Rapid lateral thickness changes of the sequence occur across synsedimentary faults (modified from Königer & Stollhofen, 2001).

https://doi.org/10.1017/S0016756802006775 Published online by Cambridge University Press

Table 1. Average geochemical composition of tuffs of the Meisenheim Formation

Tuff	Pap	Alb	Ra	Kap	Gau	Hum
Samples	10	25	15	15	10	11
SiO_2 (wt %)	72.94	72.50	74.58	71.74	70.67	75.36
TiO_2	0.19	0.06	0.07	0.15	0.19	0.14
$Al2O_3$	13.74	13.61	13.57	14.46	15.92	12.38
$Fe2O_3$	1.87	2.05	1.87	3.42	1.92	3.66
MnO	0.05	0.04	0.03	0.05	0.03	0.02
MgO	0.47	0.42	0.47	0.26	0.12	0.31
CaO	0.78	1.27	0.23	0.75	0.45	0.14
Na_2O	2.21	1.30	2.62	0.30	0.47	0.19
K_2O	3.11	3.02	3.03	3.21	5.42	2.70
P_2O5	0.15	0.06	0.07	0.07	0.05	0.07
(SO_3)	0.01	0.04	0.02	0.01	0.01	0.02
LOI	3.87	5.05	2.97	4.18	2.83	4.03
Total	99.39	99.42	99.53	98.60	98.08	99.02
Sc (ppm)	4	3	3	4	5	4
V	20	9	13	17	26	20
Cr	22	4	7	12	86	8
Co	4	4	4	8	5	5
Ni	6	5	6	9	14	8
Cu	20	19	14	32	14	43
Zn	38	31	29	30	20	123
Ga	14	16	15	8	8	8
Rb	130	98	229	59	91	42
Sr	98	42	42	34	36	44
Y	19	15	10	14	10	11
Zr	66	55	52	74	70	58
Nb	16	14	13	8	7	7
Mo	2	3	3	4	2	2
Sn	21	34	26	7	14	7
Sb	14	8	8	9	8	9
Cs	18	13	7	5	5	5
Ba	443	311	302	245	374	431
Hf	5	4	4	4	5	4
Ta	5	6	5	5	5	4
W	4	4	4	4	4	5
Pb	83	93	30	26	13	92
Bi	4	4	2	3	3	2
Th	15	14	16	11	13	11
U	11	12	7	5	6	7
La	10	6	7	9	7	9
Ce	25	14	14	23	16	19
Pr	2.82	1.67	1.79	2.57	1.60	2.25
Nd	10.79	6.13	6.26	9.86	5.75	8.16
Sm	2.58	1.70	1.51	2.14	1.17	1.64
Eu	0.36	0.18	0.20	0.31	0.19	0.29
Gd	2.47	1.65	1.34	1.93	1.09	1.41
Tb	0.50	0.37	0.29	0.34	0.22	0.25
Dy	2.76	2.22	1.69	1.90	1.17	1.35
Ho	0.51	0.43	0.33	0.37	0.23	0.27
Er	1.47	1.28	1.00	1.12	0.73	0.82
Tm	0.22	0.20	0.16	0.16	0.11	0.13
Yb	1.46	1.38	1.10	1.13	0.79	0.89
Lu	0.21	0.20	0.16	0.17	0.12	0.14

Tuffs: Pap = Pappelberg, Alb = St. Alban, Ra = Raumberg, Kap = Kappeln, Gau = Gaugrehweiler, Hum = Humberg Tuff

Formation can be easily distinguished from the various siliciclastic 'background' sediments when not admixed with detritus. The tuffs are up to 75 cm thick and some can be traced widely within the basin over at least 50 km in a NE–SW direction. Thus, these tuff beds provide important stratigraphic markers within the complex sedimentary sequence of the Saar–Nahe Basin. In Figure 3, the lithostratigraphic positions and lateral occurrences of the main tuff horizons in the southeastern part of the study area are illustrated. For their exact lithostratigraphic positions and appearances see Königer (2000) and Königer & Stollhofen (2001).

Occasionally tephrostratigraphic markers split laterally into two layers which are separated by fine-grained siliciclastic sediments (e.g. Raumberg, Gaugrehweiler, Humberg tuffs). This feature is ascribed to a differential synsedimentary subsidence of adjacent hanging wall and footwall blocks. For example, an ash layer is deposited on both sides of a synsedimentary active fault. Due to subsidence of the hanging wall blocks, the following siliciclastic sedimentation is restricted to the hanging wall blocks, whereas on the footwall blocks no siliciclastic material is deposited on top of the first ash layer. Then, a second ash layer is deposited. This leads to an 'amalga-

https://doi.org/10.1017/S0016756802006775 Published online by Cambridge University Press

mation' of the two ash layers on the footwall blocks resulting in one horizon, whereas on the hanging wall blocks two individual horizons occur separated by a siliciclastic sequence up to several metres thick.

The preservation of the volcanic ash was strongly influenced by the depositional environment. The very fine-grained ashes were deposited as distal pyroclastic fallout in essentially three different settings, each with a contrasting preservation potential (Königer & Stollhofen, 2001). (1) Tuffs interbedded with shales and siltstones in the offshore-lacustrine setting had the highest preservation potential due to lack of or only very minor reworking of the ash on the lake floor. (2) In the prodelta to delta front environment, primary ashes were partly reworked by turbidity currents or wave activity or have been admixed with siliciclastic material. (3) Tuffs interbedded with flood plain and crevasse splay sediments of the delta plain setting are often cross-bedded. In this setting, reworking was common and associated with an abundant admixture of siliciclastic detritus or even erosion of the entire ash bed.

In addition, the preservation potential was controlled by contemporaneous fault displacements. Ash beds deposited in footwall positions were strongly affected by reworking and erosion, and usually were preserved with reduced thickness only. In contrast, hanging wall blocks provided an enhanced preservation potential due to minor reworking of primary ashes and an increased redeposition of reworked ashes which have been derived from footwall blocks, for example. A descriptive summary of the pyroclastic lithofacies is given by Königer & Stollhofen (2001).

4.b. Mineralogy

Following deposition, the ash beds altered to various clay mineral assemblages. In general, the equigranular crypto- to microcrystalline quartz-kaolinite matrix of the tuff horizons contains a uniform assemblage of juvenile magmatic components. These comprise completely recrystallized platy and cuspate former glass shards up to 200 μm in diameter. Crystal components are dominated by thorn-shaped, inclusion-free solid volcanic quartz splinters up to 650 μm in size. Crystals of euhedral sanidine and marginally corroded plagioclase reach up to 500 μm in size and are usually extensively altered to kaolinite. Biotite shows euhedral crystal outlines, reaches up to 1.5 mm in diameter and contains a few apatite microlites besides abundant inclusions of zircon and monazite with dark brown pleochroic haloes. These components demonstrate the original pyroclastic nature of the tephrostratigraphic horizons which are classified as vitric tuffs. The heavy-mineral assemblage consists of mainly zircon, apatite and monazite plus minor amounts of sphene and hornblende. In addition, minor contents of partly idiomorphic tourmaline, garnet and rutile occur within primary fallout deposits. Thus, these components are interpreted to represent primary magmatic phases. No pyroclastic lithic components were found in primary deposits. However, petrographic features cannot be used to distinguish different tuff horizons. A detailed description of the mineral composition is given in Königer (1999).

5. Material and methods

5.a. Samples

The quality of samples is an important factor in the attempt to differentiate tuff beds on the basis of their chemical composition. Great care was taken in the sample selection to avoid detrital contamination in the ashes which affects analytical results. Only stratigraphically well-constrained samples showing a primary fallout character without epiclastic contamination were considered. In total, 86 tuff samples were selected for whole-rock geochemical analyses from the Pappelberg, St Alban, Raumberg, Kappeln, Gaugrehweiler and Humberg tuffs (Fig. 2).

In some samples, original SiO_2 contents have been increased by secondary silicification of the ashes after deposition. This might have resulted from precipitation of SiO_2-rich solutions seeping through the unconsolidated ash layers. In Table 1, the average geochemical compositions of the analysed tuff horizons are listed. Data of individual samples are listed in Königer (1999).

5.b. Chemical methods

Major and trace elements of most samples were determined by X-ray fluorescence (XRF)-spectrometry at the Niedersächsisches Landesamt für Bodenforschung, Hannover (Germany); a few samples (12) were analysed at the Institut für Mineralogie of the Universität Würzburg (Germany). All elements were determined from fusion discs with XRF spectrometers. Corrections were based on a calibration using the international rock standards W-2 (basalt), BE-N (basalt), GSS-6 (sediment) and GH (granite). The analytical error of major elements is 1–3% depending on the proximity to the detection limits. Detection limits of trace elements range from 2 to 10 ppm depending on the analysing laboratory. The precision errors are usually 10% but they increase to 50% if the concentrations are close to their detection limits.

Determination of the rare-earth elements (REE) of most samples was carried out by inductively coupled plasma-mass spectrometry (ICP-MS) at the Niedersächsisches Landesamt für Bodenforschung, Hannover (Germany). Additional REE analyses of seven samples were performed by ICP-MS at the Department of Earth Sciences, Memorial University of Newfoundland, St John's (Canada). The samples were analysed together with a pure quartz reagent

https://doi.org/10.1017/S0016756802006775 Published online by Cambridge University Press

blank and one or more certified geological reference standards (usually gabbro MRG-1 and basalt BR-688). Full details of the analytical procedure are given by Longerich *et al.* (1990).

Some trace elements (Y, Zr, Nb, Ba, Hf, Ta, Th) of two samples were measured by XRF at Hannover and ICP-MS at St John's, although the reliability of detected Zr, Ba and Hf contents by ICP-MS is occasionally inaccurate. A good agreement of Y, Zr, Nb and Th contents between XRF and ICP-MS analyses indicates a good reproducibility of the data. However, a consistent disagreement of Y contents between XRF and ICP-MS analyses is largely attributed to a calibration 'problem' with the XRF data due to a near universal, systematic error in the certified values of Y in geological reference material used to calibrate XRFs, and so the discrepancy is perpetuated. Y contents of less than 10 ppm are particularly affected by this calibration problem (M. Tubrett, pers. comm. 1996).

6. Geochemistry

The geochemical compositions of the examined tuff horizons (1) give hints to their tectonomagmatic origin, (2) enable comparisons with possible parental rocks of potential source regions, and (3) allow intrabasinal correlations of individual tuffs.

6.a. Influences on the original ash composition

In principle, several effects could have influenced and changed the original chemical composition of tephra deposits. Below, some of these aspects are described briefly; for further information consult Cox, Bell & Pankhurst (1979), Fisher & Schmincke (1984), Cas & Wright (1987), Hall (1987) and Wilson (1989).

Magma bodies are often heterogeneous, showing a vertical chemical and mineralogical zonation due to fractional crystallization. An eruption of such a compositionally zoned magma may lead to a reverse chemical zonation of the pyroclastic deposit or might produce compositional heterogeneity within the pyroclastic bed.

Physical fractionation of magma during explosive eruption processes within the conduit and the eruption plume, forming tephra clasts and particles of variable sizes and densities, and subaerial transport of pyroclastic material in wind-driven ash clouds, modify the tephra chemistry. Aeolian fractionation can lead to downwind changes in the chemical composition of distal ash fall deposits, connected to changes in the mineralogical composition. For example, an increase in SiO_2 is attributed to a progressive loss of crystals (plagioclase, hornblende, pyroxene, apatite, magnetite) that contain less silica than pure glass particles, which were transported further away (Sarna-Wojcicki *et al.* 1981). An ash fall deposit from a homogeneous magma batch should therefore become increasingly silicic with increasing distance from the source. In addition, varying wind directions and velocities at different heights result in ejected tephra material successively transported in different directions, depositing individual ash sheets that may reflect only parts of a magma body. However, considering the small field area in the Saar–Nahe Basin (about 1000 km^2) compared to the assumed much larger lateral distribution of the examined fallout beds over several 10 000 km^2 (Königer, 2000), aeolian fractionation is not supposed to have caused chemical variations of tuff samples within the study area.

Secondary reworking of primary tephra deposits and admixture with detrital material, such as in fluvially influenced settings, significantly changes the original composition of tephra beds. Finally, these can be strongly influenced by alteration processes. When tephra layers in various geological environments alter by subaerial weathering, hydrolysis, subaqueous alteration in lakes or swamps, hydrothermal processes, or burial diagenesis, they lose most of their identity except for minor but characteristic relics and pseudomorphic textural features. Ash composition, depositional setting, climate, pore fluid type and flow, bed thickness and heat flux influence the length of time needed to completely alter volcanic ash to a tuff (Bohor & Triplehorn, 1993).

Because of the strong degree of kaolinization of the examined acidic tuffs (see Section 4.b), only the decomposition of rhyolitic glass by kaolinization is described here. During this kind of alteration of acidic ashes Al_2O_3, CaO, total Fe_2O_3 and H_2O may be enriched, whereas SiO_2, Na_2O and K_2O are commonly depleted (Huff *et al.* 1996). Concentrations of MgO, MnO and TiO_2 are almost unaffected (Spears & Rice, 1973; Höller, Kolmer & Wirsching, 1976). Immobile elements like Sc, Zr, Sb, Hf, Nb, Y, Ga, Ce and Ta retain their initial concentrations. Relatively more reactive alkaline and calc-alkaline elements like Rb, Sr and Cs are generally mobile. Th and U do show inconsistent mobility patterns. The light REE (La–Gd) are commonly immobile, whereas the heavy REE (Tb–Lu) are generally depleted in alkaline solutions but immobile in more dilute pore fluids (Winchester & Floyd, 1977; Zielinski, 1982; Summa & Verosub, 1992).

6.b. Geochemical composition of the tuff horizons

The tuff horizons have SiO_2 contents of usually 60–82 wt %. Average Cr concentrations of 4–86 ppm indicate the acid to intermediate character of the tuffs. In granites and their volcanic equivalents, average values of only 1–5 ppm occur, whereas in ultrabasic to basic rocks Cr is strongly enriched (250–1400 ppm; Stöffler, 1963). Increased Cr contents might suggest a more intermediate host magma of some tuffs. The marked negative Eu anomaly of the tuffs (see Fig. 9) is characteristic of silicic volcanism (Bohor & Triplehorn, 1993)

https://doi.org/10.1017/S0016756802006775 Published online by Cambridge University Press

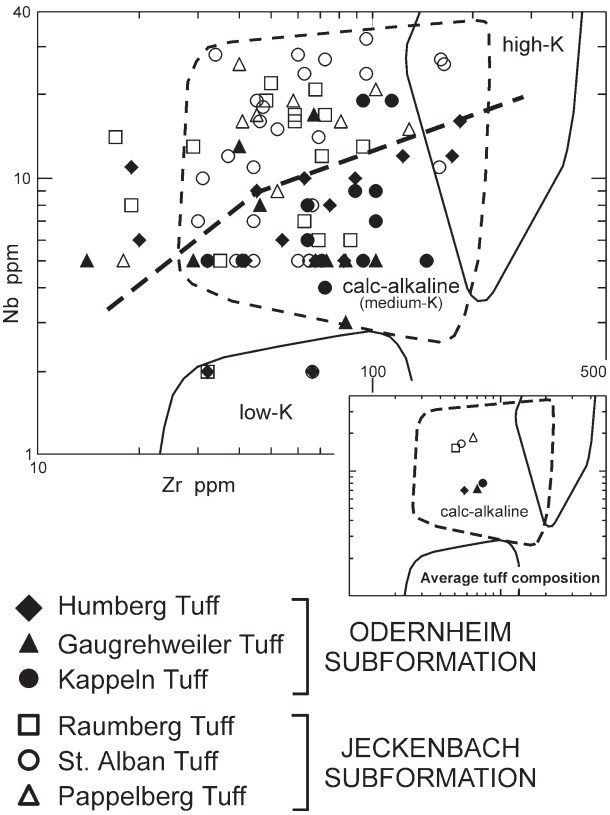

Figure 4. Classification of tuff samples in the slightly modified Nb–Zr diagram of Leat *et al.* (1986) and legend of the examined tephrostratigraphic markers of the Meisenheim Formation. Dashed line divides an area of samples predominantly of the Jeckenbach Subformation (open symbols) from an area mainly of the Odernheim Subformation (solid symbols). The detection limit of Nb is 5 ppm in most samples.

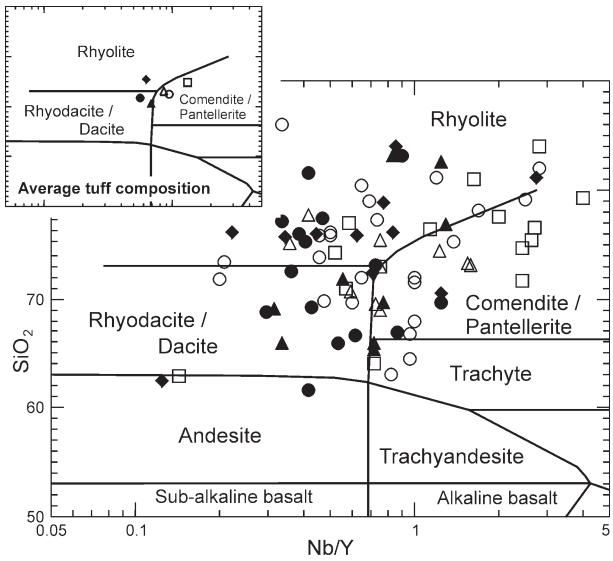

Figure 5. Classification of tuff samples in the SiO_2–Nb/Y discrimination diagram of Winchester & Floyd (1977). For tuff legend see Figure 4.

and also of highly evolved magmas in which Eu has partitioned into plagioclase during crystallization (Taylor & McLennan, 1988). In rhyolitic ashes large Eu deficiencies occur, whereas dacitic ashes have small Eu deficiencies and lower Rb concentrations than the rhyolitic ashes (Izett, 1981). The absence of a negative Ce anomaly (Fig. 9) indicates the continental–terrigenous depositional setting of the examined tuffs, whereas in marine ash tuffs a negative Ce anomaly frequently develops (Kubanek & Zimmerle, 1986).

According to Leat *et al.* (1986), the tuffs show mainly a calc-alkaline (medium-K) composition, with only a few samples plotting in the low-K and high-K fields (Fig. 4). Some samples that plot at 5 ppm Nb possibly have lower Nb contents because of a detection limit of 5 ppm for Nb in samples analysed at Würzburg (see Section 5.b). Therefore, a few more samples might plot further down toward the low-K field. This only holds true if there had been a positive correlation between Nb and K in the original geochemical composition at the source. However, a conspicuous feature is the division into a field predominantly containing samples of the stratigraphically lower Jeckenbach Subformation, showing higher Nb contents (open symbols), and a field with samples mainly of the overlying Odernheim Subformation with lower Nb concentrations (solid symbols). This is even more obvious in the plot of the average tuff compositions (inset in Fig. 4).

Within the discrimination diagram of Winchester & Floyd (1977), individual tuff samples plot preferentially in the rhyolite, rhyodacite/dacite and comendite/pantellerite fields (Fig. 5). The average tuff compositions indicate a calc-alkaline character of the ashes although high Nb/Y ratios in some samples from the Jeckenbach Subformation (open symbols) result in a plot of the average composition of the Pappelberg, St Alban and Raumberg tuffs in the (alkaline) comendite/pantellerite field (Nb/Y > 1.4).

6.c. Tectonomagmatic origin of the volcanic ash

Since the tuff horizons of the Meisenheim Formation were classified as acid to slightly intermediate, tectonic discrimination diagrams of granites can be used best to determine the tectonomagmatic derivation of the volcanic ashes, despite some deviations from the original ash composition. Most granites (and also rhyolites) are produced by partial melting of previously existing rocks but can also develop by fractional crystallization of more mafic parental magmas or even mixed magmas (Arz & Lorenz, 1996). Therefore, some aspects of the chemical composition of granites likely reflect their source material. Since the tectonic setting partly controls the type of source rocks at depth, the granite composition indirectly gives information about their tectonic setting. For this reason, tectonomagmatic discrimination diagrams such as those from

https://doi.org/10.1017/S0016756802006775 Published online by Cambridge University Press

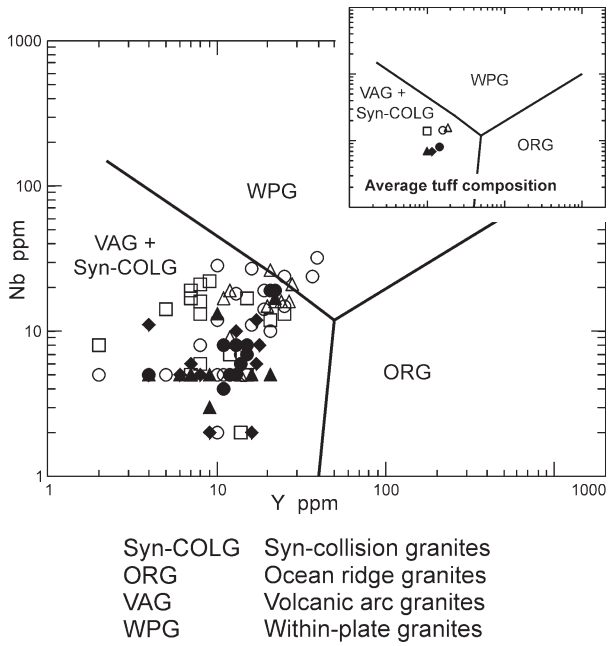

Figure 6. Classification of tuff samples within a tectonomagmatic discrimination diagram of Pearce, Harris & Tindle (1984). For tuff legend see Figure 4. The detection limit of Nb is 5 ppm in most samples.

Pearce, Harris & Tindle (1984) can be used as helpful plots for an interpretation of the tectonomagmatic origin of the examined volcanic ashes but it must be considered that these are strictly empirical diagrams and based solely on *a priori* data. Thus, these diagrams should not be subjected to rigorous interpretation.

According to Tischendorf, Förster & Trumbull (1995), overlapping of groups of granitic analyses into different fields within tectonomagmatic discrimination diagrams can be explained by the action of one or both of the following factors. First, orogenic settings are complex and many orogenic belts have a multiphase evolution. Extension within an overall compressional orogenic regime may be associated with a mixing of source regions, for example, slab and mantle wedges in back-arc basins. Second, differentiation, mixing, assimilation of magmas and alteration can produce compositional trends that can cross field boundaries within discrimination diagrams.

The granite classification of Pearce, Harris & Tindle (1984) comprises four main groups according to their intrusive settings: ocean ridge (ORG), volcanic arc (VAG), within-plate (WPG) and collision (COLG) granites. In the Nb–Y discrimination diagram almost all individual tuff sample analyses plot in the volcanic arc and syn-collision granite field (VAG + Syn-COLG; Fig. 6) whereas all average tuff compositions plot in the VAG + Syn-COLG field. A syn-collisional setting existed at the time of deposition of the ash layers in the Variscan orogen, of which the intermontane Saar–Nahe Basin is a part, whereas a volcanic arc setting was previously located at the southern margin of the Variscan orogenic belt.

Attempting further tectonomagmatic classifications of the studied altered tuff horizons by applying other diagrams is not considered advisable due to the general use of highly mobile elements like K, Na and Ca in such diagrams.

7. Source area considerations

The tectonomagmatic origin and geochemical comparisons of the Meisenheim tuffs, even of whole-rock analyses, combined with petrographic, litho- and biostratigraphic and radiometric correlations can help to determine the potential source regions of the tuff horizons of the Saar–Nahe Basin.

7.a. Regional correlation

Lateral grain-size distribution patterns of juvenile particles (e.g. zircon, quartz splinters, biotite, apatite) show in most of the tuffs a distinct increase in grain sizes toward the south (Königer *et al.* 2002). This attests to an ash derivation from areas located south of the Saar–Nahe Basin. For this reason, a source region located in southwestern England, where silicic rocks including tuffs of the same age are abundant (see e.g. Spears & Kanaris-Sotiriou, 1979), is excluded. A derivation from vents within the basin as suggested by Burger (1990) is also excluded due to a complete lack of contemporaneous magmatic or volcanic (e.g. lava flows) rocks within the Saar–Nahe Basin. In addition, grain-size comparisons of juvenile components from the Meisenheim tuffs and from various fallout deposits described in the literature suggest transport distances of the ashes of less than 400 km; even more likely are source areas within a range of 300 km (Königer *et al.* 2002).

In Central Europe, a belt of Carboniferous to Permian S-type granitoids lies within the Moldanubian section of the Variscan orogen north of the present Alps. These contrast chemically with a belt of contemporaneous, predominantly granodioritic I-type plutons in the Variscan basement thrust sheets of the Alps, corresponding to the southern flank of the Central European Variscan orogen. The regional duality of Variscan plutonism resembles the plutons along active circum-Pacific continental margins, in that there are inner S-type granitoid belts and outer I-type plutons (Finger & Steyrer, 1990). Therefore, Central Europe could have undergone a Cordilleran-type orogenic event in Late Palaeozoic time, involving northwestward subduction of the Palaeotethys ocean prior to the collision with Gondwana.

Based on the granitoid discrimination of Finger & Steyrer (1990), most tuffs of the Meisenheim Formation show an affinity to Moldanubian Variscan S-type granitoids (Fig. 7), although the average com-

https://doi.org/10.1017/S0016756802006775 Published online by Cambridge University Press

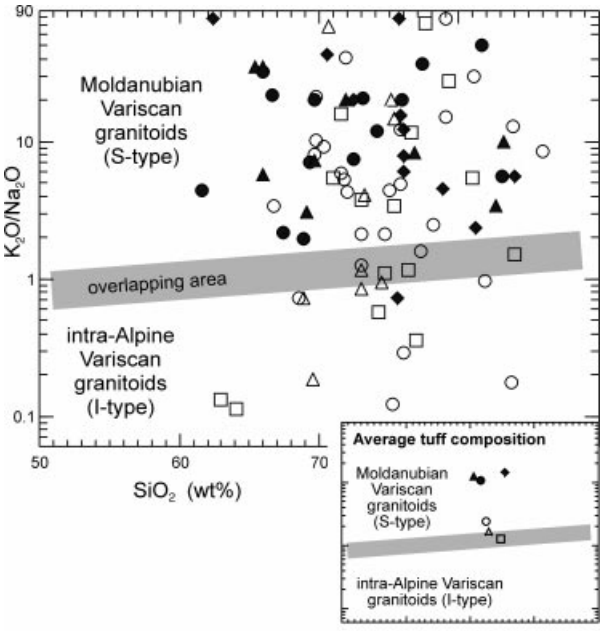

Figure 7. Classification of tuff samples within a discrimination diagram for Variscan S- and I-type granitoids in Central Europe based on Finger & Steyrer (1990). For tuff legend see Figure 4. In all probability, K and Na have been modified in the Saar–Nahe tuffs relative to their primary ash composition because of rather intensive alteration. This may have caused deviations in the K_2O/Na_2O ratio. However, an equivalent geotectonic classification based on more 'stable' elements is not yet available for the various Variscan granitoid types. For further explanations see text.

position of the Raumberg Tuff plots into the overlapping area of the S- and I-type fields. However, it has to be realized that both K and Na in all probability have been modified in the Saar–Nahe tuffs relative to their primary ash composition due to rather intensive alteration. This may have caused deviations in the K_2O/Na_2O ratio used in Figure 7. However, an equivalent geotectonic classification based on more 'stable' elements is not available yet for the various Variscan granitoid types.

The occurrence of biotite, primary muscovite and abundant monazite within the rhyolitic to rhyodacitic Saar–Nahe tuffs suggests an affiliation of these markers to highly differentiated two-mica granites and rhyolites (Königer, 1999), such as occur south and east of the Saar–Nahe Basin in the Black Forest (southwestern Germany), Vosges (eastern France) and Odenwald (Germany) (see Fig. 8).

7.b. Potential source regions

The derivation of the Meisenheim tuffs from volcanoes up to 400 km (more probably less than 300 km) south of the Saar–Nahe Basin (Königer *et al.* 2002) confines possible locations of their vents. Due to their location and distance from the Saar–Nahe Basin, the Black Forest-Vosges region and the Central Alps are especially considered to represent possible source regions where the volcanic ashes were derived from

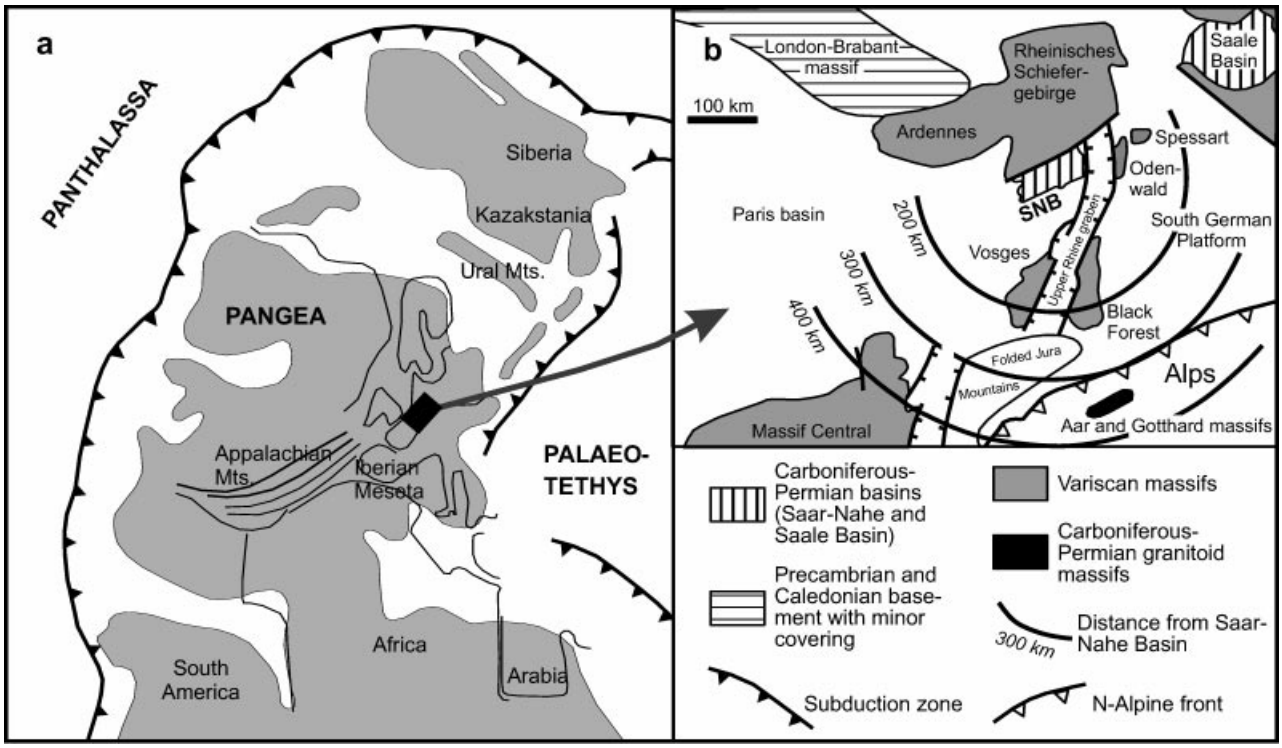

Figure 8. Location of the Saar–Nahe Basin (SNB) within (a) the palaeogeography at the Carboniferous/Permian boundary (modified from Scotese & Langford, 1995) and (b) the recent geological framework of Central Europe showing the distances of the studied tuff horizons of the Meisenheim Formation to potential source regions (exposed Variscan basement areas) (modified from Walter, 1992).

https://doi.org/10.1017/S0016756802006775 Published online by Cambridge University Press

Table 2. Geochemical comparison of the tuff horizons of the Saar-Nahe Meisenheim Formation with volcanic and pyroclastic rocks from potential source regions

	Examined tuffs	Odenwald Rhyol. rocks	Northern Black Forest Rhyol. rocks	Central Black Forest Rhyol. rocks	Central Black Forest Tuff horizons	Southern Black Forest Rhyol. rocks	Southern Black Forest Rhyodac. rocks	Vosges Ignimbrites Nideck Wisches, Donon	Vosges Rhyol. tuffs Villé Basin	Vosges Rhyolite of Blancrupt
SiO_2 (wt %)	70.67–75.36	>74	>74	70–76	68.11	< 70	68.36	< 68	77–78	74
TiO_2	0.06–0.19	0.04–0.09	0.02–0.05	0.02–0.50	0.53	0.50–0.76	0.64	0.42–0.48	0.22–0.40	0.16
Al_2O_3	12.38–15.92	11.31–13.31	11.30–13.48	12.61–14.30	15.73	14.75–14.88	15.74	14.64–15.43	10.94–12.43	12.65
Fe_2O_3	1.87–3.66	0.52–1.59	0.39–1.02	0.98–3.73	4.23	2.41–4.16	0.13	3.09–3.15	0.87–1.26	1.26
MnO	0.02–0.05	–	–	0.01–0.07	0.02	–	0.06	–	–	–
MgO	0.12–0.47	0.12–0.87	0.06–0.83	0.35–0.86	1.41	0.84–1.55	1.81	1.42–2.27	0.99–1.06	0.74
CaO	0.14–1.27	0.06–0.12	0.13–0.31	0.09–0.38	0.45	0.43–1.57	2.34	0.25–0.69	0.16–0.23	0.15
Na_2O	0.19–2.62	0.06–0.62	0.19–1.70	0.42–1.11	0.26	0.78–2.65	3.51	0.42–0.95	0.41–0.70	0.98
K_2O	2.70–5.42	6.24–8.94	4.23–9.33	7.45–8.43	5.31	5.03–7.76	4.09	6.31–7.95	3.16–4.15	7.38
P_2O_5	0.05–0.15	0.03–0.04	0.04–0.11	0.03–0.33	0.07	0.13–0.21	0.24	0.13–0.15	0.05–0.21	0.06
V (ppm)	9–26	–	0–5	10–26	66	20–50	60	50–55	45	13
Cr	6–86	–	10–20	<10	50	15–50	31	30	50	17
Ni	5–14	–	5–10	0–11	24	5–20	21	15	15	9
Rb	42–229	330–1750	580–1210	267–1094	355	240–310	159	250–280	545	470
Sr	34–98	<50 (<20)	15–20	36–260	173	60–160	358	80–95	40	59
Y	10–19	–	43	6–57	33	26	21	–	–	–
Zr	52–74	50–150 (<30)	5–45	48–525	221	230–610	243	160–165	90	93
Nb	7–16	–	14	6–32	18	9	6	–	–	–
Ba	245–443	130–420	65–170	118–1454	432	910–1670	963	445–510	150	198
La	6–10	–	50–80	<5–56	33	80–90	–	70–85	75–95	58
Ce	14–25	–	5–25	–	–	85–95	–	65–90	25–65	62
Nd	6–11	–	5–15	–	–	45–50	–	15–30	3–22	18
Data source	This study	Arikas (1986) Y and Nb by Lippolt, Schleicher & Raczek (1983)	Arikas (1986)	I. Orthmayr (unpub. Diploma thesis, Univ. Freiburg, 1986)		Arikas (1986)	Kölbl-Ebert (1992)	Arikas (1986)	Arikas (1986)	Arikas (1986)

Values give range of average contents. The listed elements are the only ones common to all data sets.

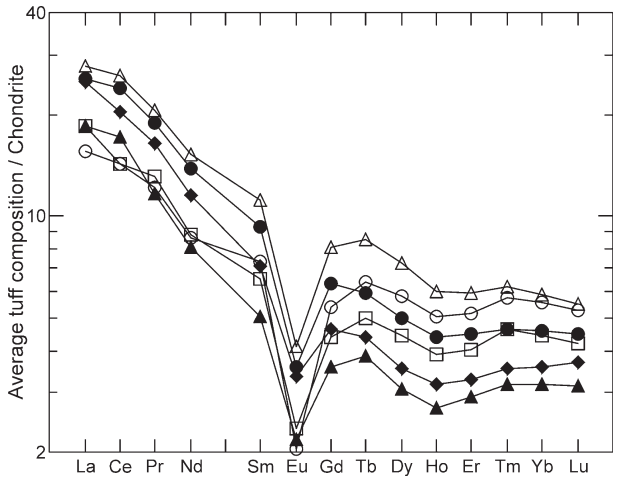

Figure 9. Chondrite-normalized rare-earth element patterns of average tuff compositions (cf. Table 1). For tuff legend see Figure 4.

(Fig. 8). This of course also applies to adjacent, geotectonically equivalent regions that are now covered by post-Palaeozoic strata. However, during deposition of the examined ash layers in the Saar–Nahe Basin, the Carboniferous–Permian granitoid massifs of the Central Alps (e.g. Aar and Gotthard massifs) have been located much further to the south than today. They reached their present location much later during the Alpine orogeny. This makes an ash origin from this region rather unlikely. An ash origin from the Massif Central in France also seems unlikely due to its distance of 400 km and more from the Saar–Nahe Basin. For this reason, the general region of the Black Forest-Vosges area is considered to be the most likely source region for the volcanic ashes (and also adjacent areas further to the west and east that are now covered by post-Palaeozoic strata).

In Table 2, a compilation of the geochemical composition of the examined tuffs and published data for magmatic rocks of potential source regions within the Odenwald–Black Forest–Vosges region is shown. The rhyolitic to rhyodacitic tuffs of the Meisenheim Formation are most similar to rhyolitic rocks of the northern and particularly of the central Black Forest, and to the Blancrupt rhyolite in the northern Vosges. This correlation applies best to TiO_2, Zr, Y, Nb, La, Ce and Nd, but V, Cr and Ni also show a good agreement. In addition, the marked negative Eu anomaly in the tuff beds of the Meisenheim Formation (Fig. 9) correlates well with REE patterns of two-mica granites from the northern and central Black Forest, whereas southern Black Forest granites do not have a negative Eu anomaly (Emmermann, Daieva & Schneider, 1975). In contrast, the Saar–Nahe tuffs show a poorer geochemical correlation with tuff horizons from both the central Black Forest and the Villé Basin in the northern Vosges. The geochemical compositions of magmatic rocks of the southern Black Forest and the Nideck–Wisches–Donon zone in the central Vosges correlate rather poorly with the tuff layers of the Meisenheim Formation (Table 2). Overall, most ashes likely derived from the region of the northern and central Black Forest and the northern Vosges (Fig. 8).

8. Chemical correlation of individual tuffs

Stratigraphic correlation of Quaternary and Holocene tephra layers frequently benefits from the use of layer-specific chemical and mineralogical information as identifying fingerprints. The underlying assumption of chemical correlation is that the discriminating elements are unique and indigenous to the original ash, and are not the product of post-depositional additions or losses (Huff *et al.* 1991). Kolata, Frost & Huff (1986, 1987) and Huff *et al.* (1991) have shown that, even after post-depositional alteration, Palaeozoic K-bentonites (tuffs) retain a chemical fingerprint of their original ash composition which allows identification and correlation on a regional scale.

8.a. Discrimination by individual elements

The utility of mobile major and trace elements for comparisons and correlations of altered tephrostratigraphic markers is commonly restricted. In contrast, incompatible trace elements are useful for comparisons. In bivariate element plots, for example in Figures 4 and 6, the overlap of data clusters from different tuff beds detracts from their use as parameters for the unequivocal correlation of individual horizons and assignment of unknown samples, and thus limits their stratigraphic value. However, some compositional differences among individual tuffs based on major and trace elements were observed, especially between groups of tuffs from the Jeckenbach and Odernheim subformations.

Tephrostratigraphic markers of the Jeckenbach Subformation (open symbols) generally have higher average Nb/Y ratios (≥ 0.8) than tuffs of the overlying Odernheim Subformation (solid symbols, ≤ 0.7). This clustering also applies to the Nb/Zr ratio (Jeckenbach Subformation ≥ 0.24, Odernheim Subformation ≤ 0.13). Similarly, tuffs of the Jeckenbach Subformation commonly have higher average concentrations of Ga (≥ 14 ppm) and Nb (≥ 13 ppm) than those from the Odernheim Subformation (Ga ≤ 8 ppm, Nb ≤ 8 ppm) (see Table 1).

With respect to metallic elements, tuffs of the Jeckenbach Subformation have a higher average Sn concentration (≥ 21 ppm) than tuffs of the Odernheim Subformation (Sn ≤ 14 ppm). In contrast, the Kappeln and Humberg tuffs of the Odernheim Subformation have the highest average Zn contents. The Gaugrehweiler Tuff shows the lowest average Pb concentration of all tuffs. According to Stimac *et al.*

https://doi.org/10.1017/S0016756802006775 Published online by Cambridge University Press

(1996), Pb concentrations often preserve magmatic values within the rocks developing from a magma. Therefore, average Pb contents of the tephrostratigraphic horizons, determined from primary ash fall deposits, can be used for discriminations between individual markers. However, extraordinarily high Pb contents, for example of more than 1000 ppm in a few samples, are ascribed to secondary influences like detrital admixing. Analyses from such samples have been removed from the data set.

As can be recognized from the examples given above, and these are the best examples from many evaluations, comparisons based on major and trace elements have only a restricted applicability and reliability for discriminations among individual tephrostratigraphic markers. Chondrite-normalized rare-earth element (REE) patterns can be used to discriminate among some horizons, at least in parts. Figure 9 shows that the Pappelberg Tuff has the highest REE concentration, and thus can be well distinguished from the Gaugrehweiler and Humberg tuffs which contain significantly lower amounts, especially in the heavy REE. Moreover, the Gaugrehweiler Tuff has generally the lowest REE contents of all tuffs (except for La and Ce). Within the St Alban Tuff concentrations of individual REE continuously increase from the light REE to the heavy REE, showing the lowest La but almost the highest Lu content of all tuffs.

8.b. Discrimination by discriminant function analysis

One of the most promising techniques for correlation and characterization of individual tuff horizons by chemical fingerprinting is discriminant function analysis, a multivariate statistical method of evaluating several elements together to determine if a distinctive chemical signature exists for each bed. Just as immobile elements serve to distinguish volcanic rocks from different magma series, the same elements should be most useful in distinguishing volcanic ashes derived from different magmas. Immobile elements are expected in juvenile minerals of (altered) volcanic ash. Kolata, Frost & Huff (1986) gave a compilation of minerals within which such immobile elements are contained.

Sometimes a single element might well serve as a good discriminator between individual beds, but a combination of elements (and element ratios) using discriminant function analysis will maximize that difference. For these elements to serve as discriminants among tuff beds, their concentrations must have been different in separate volcanic ash falls, and they must have been preserved or altered consistently in the transformation from volcanic ash to tuff. The concentrations of certain elements could have been different in the separate volcanic ash falls if the falls represented eruptions from different volcanoes or sets of volcanoes, or eruptions from individual volcanoes having a magma source that changed its chemistry over time. Statistical modelling provides a criterion by which subtle but persistent between-bed differences in chemical composition can be shown to be greater than within-bed differences, thus permitting individual beds to be distinguished from one another on a regional scale. Assumptions in the model include the equality of covariance matrices for all groups, random selection of samples, and the likely membership of unknown samples in one of the model subgroups. Geological assumptions are that tuff chemistry indicates original ash compositions, especially when considering immobile elements, and that individual beds retain their chemical identity over long distances. The chemical data of the samples were subjected to discriminant analysis to achieve the best chemical correlation of tuff beds. Discriminant analysis provides a method of handling data on a large number of elements, allows the data to be applied simultaneously, and is rigorous in respect to interpretation of the data. A detailed description of the discriminant function analysis procedure and its assumptions and limitations in respect to tuff or bentonite beds is given by Huff (1983) and Huff & Kolata (1989).

8.b.1. Statistical method

In this study, discriminant function analyses were performed on the chemical data of 86 primary tuff samples from the six main tephrostratigraphic markers of the Meisenheim Formation (see Fig. 2) using the statistical package STATISTICA. Only elements with a relatively high immobility during secondary alteration processes (see Section 6.a) were considered. The order of importance of elements and element ratios in the discriminant model was determined by numerous evaluations with the program STATISTICA. Best discrimination between tuff horizons was reached with the hierarchical ranking TiO_2, Sc, Zn, Ga, Y, Zr, Nb, Sn, Ta, Th, Nb/Y, Zr/TiO_2 and REE. This configuration is unique for the tuff discrimination in this study but possibly varies for discrimination of tuff horizons from other areas.

8.b.2. Discrimination of individual tuff horizons

The number of discriminant functions calculated is equivalent to the number of variables entered, or to one less than the number of groups (tuff horizons), whichever is smaller. In this study, three tuff horizons from both the Jeckenbach and the Odernheim subformations were compared by discriminant function analysis. In Tables 3a and 4a, the eigenvalues, corresponding canonical correlation coefficients, and Wilks' Lambda values for the two functions of the two analyses are listed. The eigenvalues, a measure of the relative amount of variance among the group of elements accounted for by each function, indicate that

https://doi.org/10.1017/S0016756802006775 Published online by Cambridge University Press

Table 3. Properties of discriminant function analysis of the tuffs of the Jeckenbach Subformation

(a)

Function	Eigenvalue	Canonical correlation	Wilks' Lambda
1	2.558851	0.847945	0.096565
2	1.909846	0.810148	0.343661

(b)

Standardized canonical discriminant function coefficients

Element (ratio) (in order of importance)	Function 1	Function 2
TiO_2	0.42644	–1.10200
Sc	0.82602	1.12014
Zn	0.55805	0.12390
Ga	–2.43475	0.94874
Y	1.00372	–1.47920
Zr	–0.52237	0.31348
Nb	–0.91101	0.06569
Sn	2.11576	–1.75367
Ta	0.92470	0.12868
Th	–1.16223	0.73090
Nb/Y	0.18022	0.02171
Zr/TiO_2	1.22425	–0.93925
La	0.07703	–0.93426
Ce	–0.16434	–1.20269
Pr	3.72618	7.83419
Nd	–8.22262	–4.37061
Sm	5.98357	–3.63557
Eu	0.77553	0.01556
Tb	–1.04562	–0.20839
Dy	–8.10117	1.95947
Ho	4.16352	3.79515
Yb	–0.68564	–4.26349
Lu	3.07014	0.74196

Table 4. Properties of discriminant function analysis of the tuffs of the Odernheim Subformation

(a)

Function	Eigenvalue	Canonical correlation	Wilks' Lambda
1	7.448532	0.938955	0.040748
2	1.904800	0.809779	0.344258

(b)

Standardized canonical discriminant function coefficients

Element (ratio) (in order of importance)	Function 1	Function 2
TiO_2	–1.1876	0.10474
Sc	–3.5655	2.21784
Zn	1.1534	–0.85503
Y	–3.8493	0.28410
Zr	–1.1661	0.39724
Nb	3.3122	0.92775
Sn	–3.5014	0.99224
Ta	0.7801	0.63789
Th	–0.4464	0.12243
Nb/Y	–1.5165	–0.24907
Zr/TiO_2	–1.0860	0.28930
La	–3.5992	–0.18143
Ce	0.3494	–0.16322
Pr	–1.5288	–2.70259
Nd	8.3013	3.25311
Sm	–5.4420	–0.51045
Eu	3.4943	–0.12345
Tb	–4.6076	1.53674
Dy	2.7397	2.05691
Ho	10.0175	–4.17305
Yb	10.6231	4.89424
Lu	–16.5103	–4.57818

the second function, although (significantly) smaller than the first, also contributes to the discriminant analyses. The canonical correlation coefficients are measures of the function's ability to discriminate among the groups. These coefficients associated with the functions show that the two discriminant functions in both analyses are each highly correlated with the groups (Huff & Kolata, 1989). Wilks' Lambda is an inverse measure of the ability to discriminate between the groups (tuffs), and can assume values between 0 (perfect discrimination) and 1 (no discrimination). Consequently, in both analyses the first function provides a good discrimination showing low values (Tables 3a, 4a). Values of the functions as calculated at the element means are given in Tables 3b and 4b (standardized canonical discriminant function coefficients). They may be considered as defining point coordinates within a two-dimensional orthogonal grid.

The territorial plots of the two discriminant analyses show that the functions effectively separate the three tuff horizons in each lithostratigraphic subformation. Almost all samples classify correctly in their respective groups, indicating that the discriminant functions are successful in achieving group or bed separation. In the Jeckenbach Subformation, a minor overlap of samples of the Raumberg Tuff with samples of the Pappelberg Tuff and St Alban Tuff, respectively, can be recognized (Fig. 10). In contrast, in the Odernheim Subformation, a good discrimination between the Kappeln, Gaugrehweiler and Humberg tuffs was achieved (Fig. 11). In the territorial plots, primary tuff samples plot rather reliably within the distribution ranges of the groups identified. This should help to identify and correlate primary tuff samples of unassigned stratigraphic position correctly to the respective tephrostratigraphic marker. A discrimination among all six tuffs within one territorial plot was not possible, even with different hierarchical rankings of elements and ratios than used for the discrimination in Figures 10 and 11.

9. Conclusions

9.a. Derivation of the volcanic ash

Although strongly altered, the tephrostratigraphic markers of the Saar–Nahe Meisenheim Formation indicate an acid to subordinated intermediate character. The commonly rhyolitic to rhyodacitic tuffs repre-

https://doi.org/10.1017/S0016756802006775 Published online by Cambridge University Press

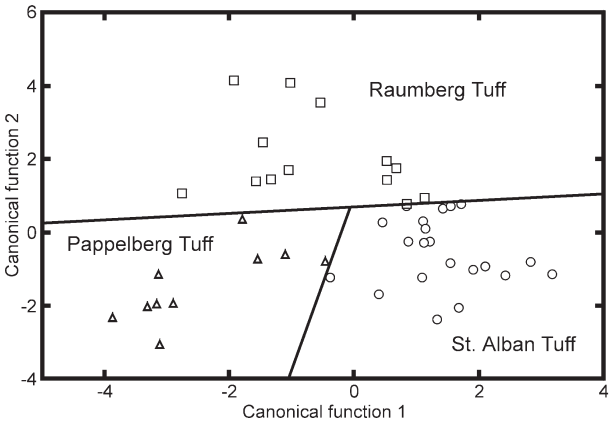

Figure 10. Territorial plot constructed for the Pappelberg, St Alban and Raumberg tuffs (Jeckenbach Subformation) from geochemical discriminant functions calculated for 23 variables (chemical elements and element ratios) of primary tuff samples (cf. Table 3). For tuff legend see Figure 4.

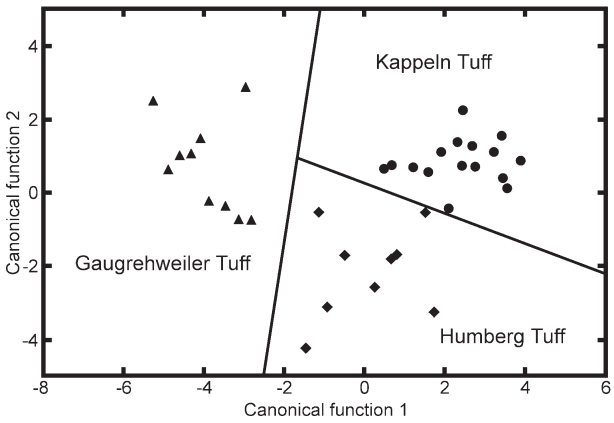

Figure 11. Territorial plot constructed for the Kappeln, Gaugrehweiler and Humberg tuffs (Odernheim Subformation) from geochemical discriminant functions calculated for 23 variables (chemical elements and element ratios) of primary tuff samples (cf. Table 4). For tuff legend see Figure 4.

sent descendants of medium- to high-K calc-alkaline magmas.

Since the chemical composition of the primary tuffs likely reflects their source material, the tectonomagmatic derivation of the volcanic ashes can be deduced. This is complicated because of the alteration of the primary volcanic ashes after deposition. However, the tuffs show an affinity to Moldanubian Variscan S-type granitoids. They probably derived from a syn-collisional setting. In consideration of petrographic (Königer, 1999), radiometric (Königer *et al.* 2002) and geochemical aspects, a principal derivation of the fall-out ashes is suggested from the region of the central and northern Black Forest (southwestern Germany) and the northern Vosges (eastern France), about 100–150 km south of the Saar–Nahe Basin. An ash origin from Carboniferous–Permian granitoid massifs in the Central Alps (e.g. Aar and Gotthard massif) or the Massif Central in France seems rather unlikely due to their greater distances from the Saar–Nahe Basin at the time of ash deposition.

9.b. Chemical fingerprinting and correlation of the tuff horizons

The widespread deposition of volcanic fallout ash is independent of the pre-eruptive topography and therefore provides the basis for useful marker horizons if the ash layers were not affected by reworking. In contrast, sandstone and black shale horizons are more or less restricted to particular parts of the basin. Due to the complex lateral and vertical sedimentary architecture of the Saar–Nahe Basin (Fig. 3) and local reworking of volcanic ash, the stratigraphic classification and correlation of tuff horizons in the field is occasionally difficult and must be supplemented with litho-, bio- and chemostratigraphic data. However, Odin, Renard & Vergnaud-Grazzini (1982) suggested the use of trace and rare-earth elements as well as isotopic ratios to establish a geochemical stratigraphy of a rock succession based on chemical comparisons and correlations of individual beds.

Here, chemical stratigraphy is applied to successive ash fall layers of the Meisenheim Formation, although separated by siliciclastic sediments. These tephrostratigraphic horizons act as useful reference levels inside the continental Saar–Nahe Basin where complex facies associations were deposited. Discriminant function analysis is the most useful tool for the study of chemical differences and to distinguish among the main tephrostratigraphic markers of the Meisenheim Formation. Within both the Jeckenbach and Odernheim subformations, three tuff horizons are well differentiated (Figs 10, 11), despite a minor data overlap of tuff samples in the Jeckenbach Subformation (Fig. 10). The chemostratigraphic identity of samples of unassigned stratigraphic position can be determined by plotting them in the discrimination diagrams.

Occasionally, the discriminant model does not provide a complete geochemical discrimination and unique identification of all beds, and some data overlap may occur (Fig. 10). Also, a discrimination of all six tuff horizons in one territorial plot was not possible. Thus, additional distinctive characteristics between individual horizons have to be considered for a unique geochemical classification of each marker or sample. Within several diagrams, such as for rock classification and tectonomagmatic discrimination or in bivariate element and REE spider plots, two or three tuffs can frequently be distinguished. For example, the Gaugrehweiler and Humberg tuffs can be distinguished by lower Pb contents of the Gaugrehweiler Tuff (Table 1). A further distinction between the St Alban and Raumberg tuffs is problematic, although the St Alban Tuff has slightly higher contents of Pb

https://doi.org/10.1017/S0016756802006775 Published online by Cambridge University Press

(Table 1) and heavy REE (Fig. 9). Moreover, tuff beds from the different subformations can be distinguished (Figs 4, 6, 7) following diagrams of Leat *et al.* (1986), Pearce, Harris & Tindle (1984) and Finger & Steyrer (1990). In addition, the St Alban Tuff is distinguished from the Gaugrehweiler and Humberg tuffs by its higher content in heavy REE (Fig. 9) and its higher Nb/Y and Nb/Zr ratios.

Within the limits of the study area, each of the tephrostratigraphic markers carries a unique and identifiable chemical fingerprint, thus allowing a reliable stratigraphic classification of samples. The results reveal that trace element fingerprinting is a viable basis for the tuff identification and correlation over a lateral distance of at least 50 km. Thus, the chemical differences between tuff beds are geologically significant and allow the establishment of a geochemical tephrostratigraphy of the Meisenheim Formation. The chemical correlation is particularly useful if combined with well-constrained litho- and biostratigraphic data. This is especially helpful in areas of complex stratigraphic and structural settings as in the continental Saar–Nahe Basin. Clearly, considerable care must be exercised in drawing conclusions based on the trace and rare-earth element chemistry of Palaeozoic tuffs, particularly because of their alteration (1) within the environment of deposition and (2) during subsequent diagenesis, possibly connected to an elevated heat flow regime in the Saar–Nahe Basin during the Early Permian (Buntebarth, 1983; Teichmüller, Teichmüller & Lorenz, 1983). A slight anchimetamorphism caused by a higher heat flow was probably connected to a widespread intrabasinal magmatic activity at the beginning of the Nahe Group (Stollhofen & Stanistreet, 1994). This possibly contributed to the alteration of the tephra deposits but such effects are usually element-specific. Königer (1999) assumed that this anchimetamorphism had only a minor influence on the alteration of the tuff horizons from the Meisenheim Formation.

However, uncertainty about alteration effects does not preclude the use of geochemical composition as a stratigraphic tool. The identification of lithostratigraphically defined tuff horizons of the Meisenheim Formation by means of completely independent geochemical criteria provides an additional basis for regional correlations of these tephrostratigraphic layers. This can be used for further studies in other regions and to establish tephrostratigraphic correlations between different Carboniferous–Permian basins in Variscan Europe.

Acknowledgements. We wish to thank all those who have contributed through their discussion to this paper, in particular H. Stollhofen (Univ. of Aachen/Germany), P. Richter (Univ. of Würzburg/Germany) and J. Haneke (Geol. Surv. of Rheinland–Pfalz/Germany). Thanks are extended to R. Hindel (Niedersächsisches Landesamt für Bodenforschung, Hannover/Germany) and M. N. Tubrett (Memorial Univ. of Newfoundland, St John's/Canada) for organizing the geochemical analyses at their institutions. Many thanks to W. D. Huff (Univ. of Cincinati/USA) for his helpful comments and the review of the initial manuscript. Editorial reviews by P. McDade, P. Leat and W. D. Huff are gratefully acknowledged. Research was funded by the Deutsche Forschungsgemeinschaft through the grant Lo 171/22-1, 2.

References

Arikas, K. 1986. Geochemie und Petrologie der permischen Rhyolithe in Südwestdeutschland (Saar–Nahe–Pfalz-Gebiet, Odenwald, Schwarzwald) und in den Vogesen. *Pollichia Buch* **8**, 321 pp.

Arz, C. & Lorenz, V. 1996. Petrogenese der Vulkanite im Saar–Nahe-Becken: Stabile und radiogene Isotope. *Terra Nostra (abstracts)* **96/2**, 11–15.

Bohor, B. F. & Triplehorn, D. M. 1993. Tonsteins: Altered volcanic-ash layers in coal-bearing sequences. *Geological Society of America Special Publication* **285**, 44 pp.

Borchardt, G. A., Harward, M. E. & Schmitt, R. A. 1971. Correlation of volcanic ash deposits by activation analysis of glass separates. *Quaternary Research* **1**, 247–60.

Borchardt, G. A., Norgren, J. A. & Harward, M. E. 1973. Correlation of ash layers in peat bogs of eastern Oregon. *Geological Society of America Bulletin* **84**, 3101–8.

Boy, J. A. & Fichter, J. 1982. Zur Stratigraphie des saarpfälzischen Rotliegenden (Oberkarbon-Unterperm; SW-Deutschland). *Zeitschrift der Deutschen Geologischen Gesellschaft* **133**, 607–42.

Boy, J. A., Meckert, D. & Schindler, T. 1990. Probleme der lithostratigraphischen Gliederung im unteren Rotliegend des Saar-Nahe-Beckens (Oberkarbon-Unterperm; SW-Deutschland). *Mainzer geowissenschaftliche Mitteilungen* **19**, 99–118.

Buntebarth, G. 1983. Zur Paläogeothermie im Permokarbon der Saar–Nahe-Senke. *Zeitschrift der Deutschen Geologischen Gesellschaft* **134**, 211–33.

Burger, K. 1990. Vulkanogene Glasscherben-Relikte in Kohlentonsteinen des Saar-Lothringer Oberkarbons sowie Herkunft und Menge der Pyroklastika. *Geologische Rundschau* **69**, 488–531.

Cas, R. A. F. & Wright, J. V. 1987. *Volcanic successions: modern and ancient*. London: Allen & Unwin, 528 pp.

Cox, K. G., Bell, J. D. & Pankhurst, R. J. 1979. *The interpretation of igneous rocks*. London: Allen & Unwin, 450 pp.

Emmermann, R., Daieva, L. & Schneider, J. 1975. Petrologic significance of rare earths distribution in granites. *Contributions to Mineralogy and Petrology* **52**, 267–83.

Finger, F. & Steyrer, H. P. 1990. I-type granitoids as indicators of a late Paleozoic convergent ocean-continent margin along the southern flank of the central European Variscan orogen. *Geology* **18**, 1207–10.

Fisher, R. V. & Schmincke, H. U. 1984. *Pyroclastic rocks*. Berlin: Springer, 472 pp.

Hall, A. 1987. *Igneous petrology*. London: Longman, 573 pp.

Haneke, J. & Kremb, K. 1998. 280 Millionen Jahre Erdgeschichte: Geowissenschaftliche Forschungen im Donnersbergkreis. *Schriftenreihe der KVH Donnersbergkreis* **2**, 3–8.

Haneke, J. & Stollhofen, H. 1994. Das lithostratigraphische

Profil der Forschungsbohrung 'Münsterappel 1'. *Mainzer geowissenschaftliche Mitteilungen* **23**, 221–8.

Harris, N. B. W., Pearce, J. A. & Tindle, A. G. 1986. Geochemical characteristics of collision-zone magmatism. In *Collision tectonics* (eds M. P. Coward and A. C. Ries), pp. 67–81. Geological Society of London, Special Publication no. 19.

Heim, D. 1960. Über die Petrographie und Genese der Tonsteine aus dem Rotliegenden des Saar-Nahe-Beckens. *Beiträge zur Mineralogie und Petrologie* **7**, 281–317.

Heim, D. 1961. Über die Tonsteintypen aus dem Rotliegenden des Saar-Nahe-Gebietes und ihre stratigraphisch-regionale Verteilung. *Notizblatt des Hessischen Landesamtes für Bodenforschung* **89**, 377–99.

Heim, D. 1970. Die Tonsteine im Unterrotliegenden des Saar–Nahe-Gebietes. *Zeitschrift der Deutschen Geologischen Gesellschaft* **120**, 297–307.

Henk, A. 1992. Mächtigkeit und Alter der erodierten Sedimente im Saar-Nahe-Becken (SW-Deutschland). *Geologische Rundschau* **81**, 323–31.

Henk, A. 1993. Subsidenz und Tektonik des Saar-Nahe-Beckens (SW-Deutschland). *Geologische Rundschau* **82**, 3–19.

Höller, H., Kolmer, H. & Wirsching, U. 1976. Chemische Untersuchungen der Umwandlung glasiger Tuffe in Montmorillonit- und Kaolinit-Minerale. *Neues Jahrbuch für Mineralogie Monatshefte* **1976/10**, 456–66.

Huff, W. D. 1983. Correlation of Middle Ordovician K-bentonites based on chemical fingerprinting. *Journal of Geology* **91**, 657–69.

Huff, W. D., Anderson, T. B., Rundle, C. C. & Odin, G. S. 1991. Chemostratigraphy, K–Ar ages and illitization of Silurian K-bentonites from the Central Belt of the Southern Uplands-Down-Longford terrane, British Isles. *Journal of the Geological Society, London* **148**, 861–8.

Huff, W. D., Bergström, S. M., Kolata, D. R. & Sun, H. 1998. The Lower Silurian Osmundsberg K-bentonite. Part II: mineralogy, geochemistry, chemostratigraphy and tectonomagmatic significance. *Geological Magazine* **135**, 15–26.

Huff, W. D. & Kolata, D. R. 1989. Correlation of K-bentonite beds by chemical fingerprinting using multivariate statistics. In *Quantitative Dynamic Stratigraphy* (ed. T. A. Cross), pp. 567–77. London: Prentice Hall.

Huff, W. D., Kolata, D. R., Bergström, S. M. & Zhang, Y.-S. 1996. Large-magnitude Middle Ordovician volcanic ash falls in North America and Europe: dimensions, emplacement and post-emplacement characteristics. *Journal of Volcanology and Geothermal Research* **73**, 285–301.

Huff, W. D., Morgan, D. J. & Rundle, C. C. 1996. Silurian K-bentonites of the Welsh Borderlands: Geochemistry, mineralogy and K–Ar ages of illitization. *British Geological Survey Technical Report* **WG/96/45**, 25 pp.

Izett, G. A. 1981. Volcanic ash beds: Recorders of Upper Cenozoic silicic pyroclastic volcanism in the Western United States. *Journal of Geophysical Research* **86**, 10200–22.

Kolata, D. R., Frost, J. K. & Huff, W. D. 1986. K-bentonites of the Ordovician Decorah Subgroup, Upper Mississippi Valley: Correlation by chemical fingerprinting. *Illinois State Geological Survey Circular* **537**, 30 pp.

Kolata, D. R., Frost, J. K. & Huff, W. D. 1987. Chemical correlation applied to K-bentonite beds in the Middle Ordovician Decorah Subgroup, upper Mississippi Valley. *Geology* **15**, 208–11.

Kolata, D. R., Huff, W. D. & Bergström, S. M. 1996. Ordovician K-bentonites of Eastern North America. *Geological Society of America Special Publication* **313**, 1–84.

Kölbl-Ebert, M. 1992. Petrographie und Geochemie der Rhyodazite/Dazite und Lamprophyre des Südschwarzwaldes. *Jahreshefte des Geologischen Landesamtes Baden-Württemberg* **34**, 239–70.

Königer, S. 1999. *Distal ash tuffs in the lowermost Permian of the Saar-Nahe Basin (SW-Germany): Distribution, sedimentology, volcanology, petrography, geochemistry, and zircon ages*. Published Dr. rer. nat. thesis, Universität Würzburg, Germany, 269 pp.

Königer, S. 2000. Verbreitung, Fazies und stratigraphische Bedeutung distaler Aschentuffe der Glan-Gruppe im karbonisch-permischen Saar–Nahe-Becken (SW-Deutschland). *Mainzer geowissenschaftliche Mitteilungen* **29**, 97–132.

Königer, S., Lorenz, V., Stollhofen, H. & Armstrong, R. A. 2002. Origin, age and stratigraphic significance of distal fallout ash tuffs from the Carboniferous–Permian continental Saar–Nahe Basin (SW-Germany). *International Journal of Earth Sciences (Geologische Rundschau)* **91**, 341–56.

Königer, S. & Stollhofen, H. 2001. Environmental and tectonic controls on preservation potential of distal fallout ashes in fluvio-lacustrine settings: The Permo-Carboniferous Saar–Nahe Basin, SW-Germany. In *Volcaniclastic Sedimentation in Lacustrine Settings* (eds J. D. L. White and N. Riggs), pp. 263–84. International Association of Sedimentologists, Special Publication no. 30.

Königer, S., Stollhofen, H. & Lorenz, V. 1995. Tuff layers in the 'Lower Rotliegend' (Lebach-Group) of the Saar–Nahe Basin (SW-Germany): Occurences, sedimentation patterns, and significance. *Terra Nostra* **7**, 79–83.

Kubanek, F. & Zimmerle, W. 1986. Tuffe und kieselige Tonschiefer aus dem tieferen Unterkarbon der Bohrung Adlersberg (West-Harz). *Geologisches Jahrbuch* **D78**, 207–68.

Leat, P. T., Jackson, S. E., Thorpe, R. S. & Stillman, C. J. 1986. Geochemistry of bimodal basalt-subalkaline/peralkaline rhyolite provinces within the Southern British Caledonides. *Journal of the Geological Society, London* **143**, 259–73.

Lippolt, H. J. & Hess, J. C. 1989. Isotopic evidence for the stratigraphic position of the Saar-Nahe-Rotliegend volcanism. III. Synthesis of results and geological implications. *Neues Jahrbuch für Geologie und Paläontologie Monatshefte* **1989/9**, 553–9.

Lippolt, H. J., Hess, J. C. & Burger, K. 1984. Isotopische Alter von pyroklastischen Sanidinen aus Kaolin-Kohlentonsteinen als Korrelationsmarken für das mitteleuropäische Oberkarbon. *Fortschritte in der Geologie von Rheinland und Westfalen* **32**, 119–50.

Lippolt, H. J., Schleicher, H. & Raczek, I. 1983. Rb–Sr systematics of Permian volcanites in the Schwarzwald (SW-Germany). Part I: Space of time between plutonism and late orogenic volcanism. *Contributions to Mineralogy and Petrology* **84**, 272–80.

Longerich, H. P., Jenner, G. A., Fryer, B. J. & Jackson, S. E. 1990. Inductively coupled plasma-mass spectrometry analysis of geological samples; a critical evaluation based on case studies. *Chemical Geology* **83**, 105–18.

Lorenz, V. & Nicholls, I. A. 1976. The Permocar-

boniferous basin and range province of Europe. An application of plate tectonics. In *The continental Permian in Central, West, and South Europe* (ed. H. Falke), pp. 313–42. Dordrecht: Reidel.

Lorenz, V. & Nicholls, I. A. 1984. Plate and intraplate processes of Hercynian Europe during the Late Paleozoic. *Tectonophysics* **107**, 25–56.

Menning, M. 1995. A numerical time scale for the Permian and Triassic periods: An integrated time analysis. In *The Permian of Northern Pangea, Vol. 1* (eds P. A. Scholle, T. M. Peryt and D. S. Ulmer-Scholle), pp. 77–97. Berlin: Springer.

Menning, M., Weyer, D., Drozdzewski, G. & van Ameron, H. W. J. 1997. Carboniferous time scales – Revised 1997 time scale A (min. ages) and time scale B (max. ages) – Use of geological time indicators. *Carboniferous Newsletter* **15**, 26–8.

Odin, G. S., Renard, M. & Vergnaud-Grazzini, C. 1982. Geochemical events as a means of correlation. In *Numerical dating in stratigraphy, Part 1* (ed. G. S. Odin), pp. 37–71. New York: John Wiley.

Pearce, J. A., Harris, N. B. W. & Tindle, A. G. 1984. Trace element discrimination diagrams for the tectonic interpretation of granitic rocks. *Journal of Petrology* **25**, 956–83.

Randle, K., Goles, G. G. & Kittleman, L. R. 1971. Geochemical and petrological characterization of ash samples from Cascade Range volcanoes. *Quaternary Research* **1**, 261–82.

Sarna-Wojcicki, A. M., Meyer, C. E., Woodward, M. J. & Lamothe, P. J. 1981. Composition of air-fall ash erupted on May 18, May 25, June 12, July 22, and August 7. In *The 1980 eruptions of Mount St. Helens, Washington* (eds P. W. Lipman and D. R. Mullineaux), pp. 667–81. United States Geological Survey Special Paper 1250.

Scotese, C. R. & Langford, R. P. 1995. Pangea and the paleogeography of the Permian. In *The Permian of Northern Pangea, Vol. 1* (eds P. A. Scholle, T. M. Peryt and D. S. Ulmer-Scholle), pp. 3–19. Berlin: Springer.

Spears, D. A. & Kanaris-Sotiriou, R. 1979. A geochemical and mineralogical investigation of some British and other European tonsteins. *Sedimentology* **26**, 407–25.

Spears, D. A. & Rice, C. M. 1973. An Upper Carboniferous tonstein of volcanic origin. *Sedimentology* **20**, 281–94.

Stimac, J., Hichmott, D., Abell, R., Larocque, A. C. L., Broxton, D., Gardner, J., Chipera, S., Wolff, J. & Gauerke, E. 1996. Redistribution of Pb and other volatile trace metals during eruption, devitrification, and vapor-phase crystallization of the Bandelier Tuff, New Mexico. *Journal of Volcanology and Geothermal Research* **73**, 245–66.

Stöffler, D. 1963. Neuere Erkenntnisse in der Tonsteinfrage aufgrund sedimentpetrographischer und geochemischer Untersuchungen im Flöz Wahlschied der Grube Ensdorf (Saar). *Beiträge zur Mineralogie und Petrographie* **9**, 285–312.

Stollhofen, H. 1998. Facies architecture variations and seismogenic structures in the Carboniferous–Permian Saar–Nahe Basin (SW-Germany): evidence for extension-related transfer fault activity. *Sedimentary Geology* **119**, 47–83.

Stollhofen, H. & Stanistreet, I. G. 1994. Interaction between bimodal volcanism, fluvial sedimentation and basin development in the Permo-Carboniferous Saar–Nahe Basin (southwest Germany). *Basin Research* **6**, 245–67.

Summa, L. L. & Verosub, K. L. 1992. Trace element mobility during early diagenesis of volcanic ash: Applications to stratigraphic correlation. *Quaternary International* **13/14**, 149–57.

Taylor, S. R. & McLennan, S. M. 1988. The significance of the rare earths in geochemistry and cosmochemistry. In *Handbook on the physics and chemistry of rare earths* (eds K. A. Gschneider and L. Eyring), pp. 485–578. New York: Elsevier.

Teichmüller, M., Teichmüller, R. & Lorenz, V. 1983. Inkohlung und Inkohlungsgradienten im Permokarbon der Saar–Nahe-Senke. *Zeitschrift der Deutschen Geologischen Gesellschaft* **134**, 153–210.

Tischendorf, G., Förster, H.-J. & Trumbull, R. B. 1995. Evaluation of trace element tectonic discrimination diagrams for silicic igneous rocks. *Terra Nostra* **7**, 137–40.

Walter, R. 1992. *Geologie von Mitteleuropa*. Stuttgart: Schweizerbart, 561 pp.

Westgate, J. A., Christiansen, E. Q. & Boellstorff, J. D. 1977. Wascana Creek ash (Middle Pleistocene) in southern Saskatchewan: characterization, source, fission track age, paleomagmatism, and stratigraphic significance. *Canadian Journal of Earth Sciences* **14**, 357–74.

Westgate, J. A. & Fulton, J. J. 1975. Tephrostratigraphy of Olympia interglacial sediments in south-central British Columbia, Canada. *Canadian Journal of Earth Sciences* **12**, 489–502.

Wilson, M. 1989. *Igneous Petrogenesis*. London: Chapman & Hall, 466 pp.

Winchester, J. A. & Floyd, P. A. 1977. Geochemical discrimination of different magma series and differentiation products using immobile elements. *Chemical Geology* **20**, 325–43.

Ziegler, P. A. 1990. *Geological Atlas of Western and Central Europe*. Den Haag: Geological Society Publication House, 239 pp.

Zielinski, R. A. 1982. The mobility of uranium and other elements during alteration of rhyolite ash to montmorillonite: a case study in the Troublesome Formation, Colorado, USA. *Chemical Geology* **35**, 185–204.